

MIT Open Access Articles

Rate coefficients and kinetic isotope effects of the $X + CH_4 \rightarrow CH_3 + HX$ ($X = H, D, Mu$) reactions from ring polymer molecular dynamics

The MIT Faculty has made this article openly available. **Please share** how this access benefits you. Your story matters.

Citation: Li, Yongle, Yury V. Suleimanov, Jun Li, William H. Green, and Hua Guo. "Rate Coefficients and Kinetic Isotope Effects of the $X + CH_4 \rightarrow CH_3 + HX$ ($X = H, D, Mu$) Reactions from Ring Polymer Molecular Dynamics." *The Journal of Chemical Physics* 138, no. 9 (2013): 094307.

As Published: <http://dx.doi.org/10.1063/1.4793394>

Publisher: American Institute of Physics (AIP)

Persistent URL: <http://hdl.handle.net/1721.1/92370>

Version: Author's final manuscript: final author's manuscript post peer review, without publisher's formatting or copy editing

Terms of use: Creative Commons Attribution-Noncommercial-Share Alike



Rate coefficients and kinetic isotope effects of the $X + CH_4 \rightarrow CH_3 + HX$ ($X = H, D, Mu$) reactions from ring polymer molecular dynamics

Yongle Li,^{1,#} Yury V. Suleimanov,^{2,#,} Jun Li,¹ William H. Green,² and Hua Guo^{1,*}*

*¹Department of Chemistry and Chemical Biology, University of New Mexico,
Albuquerque, NM 87131, USA*

*²Department of Chemical Engineering, Massachusetts Institute of Technology,
Cambridge, MA 02139, USA*

#: Equally contributed to this work.

*: Corresponding authors. Emails: ysuleyma@mit.edu, hguo@unm.edu

Abstract

The thermal rate coefficients and kinetic isotope effects have been calculated using ring polymer molecular dynamics (RPMD) for the prototypical reactions between methane and several hydrogen isotopes (H, D, and Mu). The excellent agreement with the theoretical rate coefficients of the H + CH₄ reaction obtained previously from a multi-configuration time-dependent Hartree (MCTDH) calculation on the same potential energy surface provides strong evidence for the accuracy of the RPMD approach. These quantum mechanical rate coefficients are also in good agreement with the results obtained previously using the transition-state theory with semi-classical tunneling corrections for the H/D + CH₄ reaction reactions. However, it is shown that the RPMD rate coefficients for the ultralight Mu reaction with CH₄ are significantly smaller than the experimental data, presumably suggesting inaccuracies in the potential energy surface. Significant discrepancies between the RPMD and transition-state theory results have also been found for this challenging system.

Keywords: tunneling, combustion, quantum dynamics, path integral, transition-state theory

I. Introduction

The abstraction reaction between hydrogen atom and methane, $\text{H} + \text{CH}_4 \rightarrow \text{H}_2 + \text{CH}_3$, has attracted much interest because of its importance in combustion chemistry.¹ The rate coefficient of the reaction is well known over a large temperature range.²⁻⁸ It has also served as a benchmark for understanding bimolecular reaction dynamics involving polyatomic molecules.⁹⁻¹¹ Due to the involvement of light hydrogenic atoms, the reaction is intrinsically quantum mechanical. Quantum effects, such as tunneling and zero-point energy (ZPE), manifest not only in dynamics, but also in kinetics as well. Indeed, large and inverse kinetic isotopic effects (KIEs) have been observed for this important prototypical reaction.^{3,5}

An exact quantum mechanical account of the dynamics of this twelve-dimensional reaction poses a formidable challenge.¹² As a pre-requisite, a globally accurate potential energy surface (PES) has to be developed based on high-level *ab initio* calculations.¹³ Much progress has been made in this aspect and several such PESs have been reported for the title reaction.¹⁴⁻²¹ However, a full-dimensional quantum mechanical treatment of the reaction dynamics is still very difficult. With the exception of the multi-dimensional time-dependent Hartree²²⁻²³ (MCTDH) calculations,²⁴⁻³⁵ most quantum dynamical studies of this reaction have been cast in reduced-dimensional models,³⁶⁻⁴⁵ due to the exponential scaling laws of CPU and memory requirements. Even in the MCTDH work, the *J*-shifting approximation⁴⁶ had to be used in order to make the calculations feasible. Nonetheless, the MCTDH results has remained as the most accurate quantum treatment and provide the benchmarks for all approximate models.⁴⁷

For the rate coefficients and kinetic isotope effects, it is not necessary to understand the complete reaction dynamics, as the state-to-state scattering attributes are averaged by the Boltzmann factor. Indeed, the transition-state theory (TST) offers a direct and more efficient theoretical approach for calculating rate coefficients.⁴⁸ To include quantum effects, many semi-classical models have been proposed,⁴⁹⁻⁵⁰ including the well-established small-curvature tunneling (SCT), large-curvature tunneling (LCT), and the microcanonical optimized multidimensional tunneling (μ OMT) methods. However, these semi-classical approximations, which have seldom been tested for large systems due to the lack of accurate full-dimensional quantum studies, may not provide reliable results in the deep tunneling regime because the tunneling is inherently multi-dimensional. Another uncertainty in the TST approach is the effect of recrossing near the transition state. While the variational transition-state theory can reduce the impact of recrossing,⁵¹ it is hard to quantify the error due to the neglect of this factor. The thermal rate coefficients of the reactions between methane and various isotopes of hydrogen (H, D, T, and Mu) have been computed using both variational TST with semi-classical treatments of tunneling^{18, 52-55} and MCTDH.^{24-30, 32, 34-35} (Here, Mu, denoting muonium, is a short-lived ultralight hydrogen isotope with a mass of 0.113 au). While agreement between semi-classically corrected TST and MCTDH results has generally been quite good,⁵² significant disagreement with experimental KIEs has been found.^{18, 29, 42, 53} Since KIEs are more sensitive to the details of the PES, these discrepancies suggest possible errors either in the PES or the theoretical methods themselves. To this end, Pu and Truhlar have compiled a list of possible reasons for the experiment-theory discrepancies,⁵³ but a clear identification of the origin remains elusive. Some of the possible reasons are related to

the uncertain validity of the approximate methods used to obtain the theoretical rate coefficients, which we hope to rule out by the calculations presented in this work.

To this end, we present here a ring polymer molecular dynamics (RPMD) study of rate coefficients of the title reactions and kinetic isotope effects using the recently developed RPMDrate code.⁵⁶ RPMD is an approximate quantum theory based on the isomorphism between quantum statistical properties and classical mechanics.⁵⁷⁻⁵⁸ To this end, each quantum particle is represented by a ring polymer made up of a number of beads connected with harmonic potentials. The advantage of RPMD in computing thermal rate coefficients is two-fold. First, it is a full-blown albeit approximate quantum dynamical theory that takes into consideration zero-point energy, recrossings and tunneling, which are important for the KIEs. Second, its implementation with classical trajectories gives its much more attractive scaling laws than MCTDH. In fact, most chemical reactions can be studied using RPMD with only about 1-2 order of magnitude higher computational costs than conventional quasi-classical trajectory (QCT) calculations. Recent applications of RPMD in rate coefficient calculations of bimolecular reactions,^{56, 59-63} including those for the H + CH₄ reaction,^{56, 60} have demonstrated its accuracy, even in the deep tunneling regime.⁶⁴ In this work, the RPMD rate coefficients for the title reactions and KIEs were generated using a recent *ab initio* calibrated empirical PES,¹⁷ on which TST¹⁸ and MCTDH calculations³⁴ have been reported. Comparison with these earlier theoretical results sheds light on the accuracy of various theoretical methods, and comparison with experiment yields insight on the reliability of the PES. This publication is organized as follows. The RPMD method is outlined in the

next section (Sec. II), followed by computational details (Sec. III). The results are presented and discussed in Sec. IV, and conclusions are given in Sec. V.

II. Method

All calculations are performed using the recently developed RPMDrate code.⁵⁶ Only a brief description of computational methodology used in the current work is given here. For more detailed derivations of some of the working equations we refer the reader to Refs. 60 and 56. For the six-atom molecular system, the Hamiltonian can be written in atomic Cartesian coordinates as follows:

$$\hat{H} = \sum_{i=1}^6 \frac{|\hat{\mathbf{p}}_i|^2}{2m_i} + V(\hat{\mathbf{q}}_1, \hat{\mathbf{q}}_2, \dots, \hat{\mathbf{q}}_6), \quad (1)$$

where $\hat{\mathbf{p}}_i$ and $\hat{\mathbf{q}}_i$ are the momentum and position operators of the i_{th} atom, and the m_i is its atomic mass. Taking advantage of the classical isomorphism between the quantum system and the ring polymer, each quantum particle is represented by a necklace with n classical beads connected by a harmonic potential.⁵⁷⁻⁵⁸

$$H_n(\mathbf{p}, \mathbf{q}) = \sum_{i=1}^6 \sum_{j=1}^n \left(\frac{|\mathbf{p}_i^{(j)}|^2}{2m_i} + \frac{1}{2} m_i \omega_n^2 |\mathbf{q}_i^{(j)} - \mathbf{q}_i^{(j-1)}|^2 \right) + \sum_{j=1}^n V(\mathbf{q}_1^{(j)}, \mathbf{q}_2^{(j)}, \dots, \mathbf{q}_6^{(j)}), \quad (2)$$

where $\mathbf{q}_i^{(0)} = \mathbf{q}_i^{(n)}$ and the force constant between adjacent beads is given by $\omega_n = (\beta_n \hbar)^{-1}$

with the reciprocal temperature of the system $\beta_n = \frac{n}{k_B T}$.

To obtain the reaction coordinate for the title reaction, two dividing surfaces are first defined in terms of the ring-polymer centroids. The first dividing surface is placed in the reactant asymptote:

$$s_0(\bar{\mathbf{q}}) = R_\infty - |\bar{\mathbf{R}}|, \quad (3)$$

where $|\bar{\mathbf{R}}|$ is the centroid of the vector that connects the centers of mass of the reactants and R_∞ is an adjustable parameter. In practice, it is chosen to be sufficiently large to make the interaction negligible between the reactants. The second dividing surface is placed in the transition-state region and is defined in terms of the bond-breaking and bond-forming distances as discussed in Ref. 56. The title system has one bond that forms and breaks in the reaction and four equivalent product arrangement channels:⁶⁰

$$s_1(\bar{\mathbf{q}}) = \max \{s_{1\alpha}(\bar{\mathbf{q}}), s_{1\beta}(\bar{\mathbf{q}}), s_{1\gamma}(\bar{\mathbf{q}}), s_{1\delta}(\bar{\mathbf{q}})\}, \quad (4)$$

where

$$s_{1x}(\bar{\mathbf{q}}) = \left(|\bar{\mathbf{q}}_{\text{CH}_x}| - q_{\text{CH}_x}^\# \right) - \left(|\bar{\mathbf{q}}_{\text{HH}_x}| - q_{\text{HH}_x}^\# \right). \quad (5)$$

Here $\bar{\mathbf{q}}_{\text{AB}}$ denotes the vector that connects the centroids of atoms A and B, H' denotes the reactant hydrogen isotope and $q_{\text{AB}}^\#$ is the corresponding interatomic distance at the transition state saddle point.

The reaction coordinate ξ is defined as an interpolation that connects these dividing surfaces^{56, 59-60}

$$\xi(\bar{\mathbf{q}}) = \frac{s_0(\bar{\mathbf{q}})}{s_0(\bar{\mathbf{q}}) - s_1(\bar{\mathbf{q}})} \quad (6)$$

such that $\xi \rightarrow 0$ as $\mathfrak{s}_0 \rightarrow 0$ and $\xi \rightarrow 1$ as $\mathfrak{s}_1 \rightarrow 0$.

The initial RPMD rate theory relied on the direct computation of the flux-side correlation function,⁶⁵ which requires the reactant partition function.⁶⁶⁻⁶⁷ The partition

function can be quite difficult to compute accurately, particularly for polyatomic reactants such as in the title reaction.²⁶ To avoid the direct computation of the partition function, the Bennett-Chandler factorization^{68,69} is used:^{56, 59-60}

$$k_{\text{RPMD}} = k_{\text{QTST}}(T; \xi^\ddagger) \kappa(t \rightarrow \infty; \xi^\ddagger). \quad (7)$$

The first factor in the above equation represents the static contribution while the second factor is the dynamical correction. This approach is particularly suited for activated reactions as barrier crossing is a rare event.⁷⁰⁻⁷¹

In particular, $k_{\text{QTST}}(T; \xi^\ddagger)$ is the centroid-density quantum transition-state theory (QTST) rate coefficient,^{67, 72} evaluated at the top of the free energy barrier, ξ^\ddagger , along the reaction coordinate $\xi(\mathbf{q})$, which might or might not coincide with the dividing surface $s_1 = 0$ ($\xi = 1$). This quantity depends on the position of the dividing surfaces and is determined entirely by static equilibrium properties. In practice, it is calculated from the centroid potential of mean force (PMF):^{56, 59-60}

$$k_{\text{QTST}}(T, \xi^\ddagger) = 4\pi R_\infty^2 \left(\frac{1}{2\pi\beta\mu_{\text{R}}} \right)^{1/2} e^{-\beta[W(\xi^\ddagger) - W(0)]}, \quad (8)$$

where μ_{R} is the reduced mass between the two reactants and $W(\xi^\ddagger) - W(0)$ is the free-energy difference which is obtained via umbrella integration along the reaction coordinate.^{56, 73}

The dynamical correction is provided by the second factor ($\kappa(t \rightarrow \infty; \xi^\ddagger)$) in Eq. (7), which is the long-time limit of a time-dependent ring-polymer transmission coefficient. It is expressed as the ratio between two flux-side correlation functions:

$$\kappa(t \rightarrow \infty; \xi^\ddagger) = \frac{c_{fs}^{(n)}(t \rightarrow \infty; \xi^\ddagger)}{c_{fs}^{(n)}(t \rightarrow 0_+; \xi^\ddagger)} \quad (9)$$

accounting for recrossing at the transition state (ξ^\ddagger). The transmission coefficient, $\kappa(t; \xi^\ddagger)$, reaches a plateau relatively quickly, and no long-time propagation is needed. It has been pointed out that this factor counterbalances $k_{\text{QTST}}(T; \xi^\ddagger)$, ensuring that the RPMD rate coefficient $k_{\text{RPMD}}(T)$ is independent of the choice of the dividing surface.⁶⁷ In practice, the transmission coefficient is calculated by sampling ring-polymer trajectories starting with their centroid pinned at ξ^\ddagger .^{56, 59-60}

An added advantage of the RPMD rate theory is that it reduces to the classical limit when only one bead is used. In this limit, the static and dynamical components of Eq. (9) become identical to the classical transition-state theory rate coefficient and the classical transmission coefficient, respectively.⁵⁹ These quantities thus establish the limit to which the quantum effects such as ZPE and tunneling can be evaluated by using more beads. The minimal number of beads needed to account for the quantum effects can be estimated by the following formula:⁷⁴

$$n_{\min} \equiv \beta \hbar \omega_{\max}, \quad (10)$$

where ω_{\max} is the largest frequency of the system.

III. Computational details

The analytical PES used in this work is due to Corchado, Bravo, and Espinosa-García (PES-2008), which was calibrated with high-level *ab initio* data and is symmetric for hydrogen permutation.¹⁷ This PES was chosen because of its numerical efficiency and the existence of tunneling corrected TST¹⁸ as well as MCTDH calculations,³⁴ which indicated a good agreement with experiment. RPMD calculations have also been reported for the H + CH₄ reaction on this PES, but only at 300 K.⁵⁶ Comparison with the converged Shepard interpolated PES developed by Wu *et al.*¹⁶ indicated that this PES is very accurate for the H + CH₄ rate coefficients.³²

All calculations were performed using the recently developed RPMDrate code.⁵⁶ In this work, the thermal rate coefficients for the H/D/Mu + CH₄ reactions were calculated at the range of 200-821 K. The calculations were first done with one bead, which provides the classical limit. The number of beads was then increases until convergence. Due to the small mass of Mu, the number of beads needed to converge the rate coefficients is particularly large. However, the largest number (128) used in our calculations is significantly smaller than that reported in the recent RPMD calculations on the Mu + H₂ reaction (512).^{61, 63}

In the calculation of the PMF using umbrella sampling, different sized windows were used for the H/D + CH₄ reactions. As shown by us recently,⁶² the relatively flat PMF in the entrance channel affords a larger window size. In the entrance channel, ($-0.05 \leq \xi \leq 0.75$) a larger interval and smaller force constant were thus used, ($d\xi = 0.08$ and $k = 0.32$ (T/K) eV). Near the TS ($0.76 \leq \xi \leq 1.05$), on the other hand, a smaller interval and

larger force constant ($d\zeta=0.01$ and $k=2.72$ (T/K) eV) were used. For the Mu + CH₄ reaction, the behavior of the PMF is different and 117 windows with the same small interval ($d\zeta=0.01$) along the entire reaction coordinate range ($-0.05 \leq \zeta \leq 1.10$) were used.

In each sampling window, the system was first equilibrated for 20 ps, followed by a production run (5 ns for H/D + CH₄ and 10 ns for Mu + CH₄ split into 100 and 200 sampling trajectories, respectively) in the presence of a thermostat (generalized Langevin equation (GLE)⁷⁵ for H/D + CH₄ and Andersen thermostat⁷⁶ for Mu + CH₄). The ring-polymer equations of motion were integrated in Cartesian coordinates using a velocity Verlet integrator, as implemented in the RPMDrate code,⁵⁶ with a time step of 0.1 fs.

After the barrier position (ζ^\ddagger) is determined from the PMF calculation at each temperature, the transmission coefficients are computed at this position. This was initiated by running a long (20 ns) mother trajectory with the ring-polymer centroid fixed at the new dividing surface using the SHAKE algorithm.^{56,77} Configurations are sampled once every 2 ps to serve as the initial positions for the child trajectories used to compute the flux-side correlation functions. For each initial position, 50 separate trajectories are spawned with different initial momenta sampled from the Boltzmann distribution. These trajectories were then propagated with no constraint for 0.1 ps where the transmission coefficients reach plateau values. As in the PMF calculations, the time step is set to 0.1 fs. The parameters used in our calculations were checked to be sufficient to converge RPMD rate coefficients to within a statistical error of $\sim 5\%$.

IV. Results and Discussion

The involvement of hydrogen and its isotopes in the title reaction renders these systems strongly quantum mechanical. The number of beads required in the RPMD calculations of the rate coefficients depends on the isotope and temperature, as listed in Table 1. These numbers are not much more than the minima suggested in Eq. (10), underscoring the fast convergence of the RPMD approach.

In Fig. 1, PMFs for the H/D/Mu + CH₄ reactions at 626 K are displayed. The converged RPMD free-energy barrier heights are *lower* than the classical counterparts for H and D isotopes, obtained with a single bead. This difference can be intuitively understood as a consequence of tunneling, which lowers the free-energy barriers. Interestingly, the RPMD barrier for D is slightly *lower* than that for H at the same temperature, indicating that factors other than tunneling, particularly the vibrational frequencies near the transition state, also influence the free-energy of activation.

Interestingly, the RPMD free-energy barrier is significantly *higher* than in the classical limit in the case of the ultralight isotope Mu. This seemingly surprising behavior has also been observed in the Mu + H₂ reaction,^{61, 63} and can be attributed to the large ZPE of the MuH product relative to the reactant.⁷⁸ Indeed, it was well established that the inclusion of the ZPE results in the shifting and broadening of the vibrationally adiabatic potential, which inhibit tunneling.^{61, 63, 78-79} Apparently, the same mechanism is operative in this case. Indeed, as shown in Fig. 3, which depicts the MEP and the corresponding adiabatic curves of ground vibrational state, the H + CH₄ reaction is near thermoneutral ($\Delta H^0 \sim -0.2$ kcal/mol), while the Mu + CH₄ reaction is endothermic ($\Delta H^0 \sim 7.3$ kcal/mol)

due to the large MuH ZPE.⁵ Furthermore, the latter reaction has a much higher energy barrier, which is also shifted toward the product side. As shown in Table 1, the barrier position (ξ^\ddagger) for the Mu + CH₄ reaction is systematically larger than that of the H/D + CH₄ reactions. The effect on tunneling can also be understood in terms of the skew angle of these reactions, which is 47°, ~~and 38°, and 72°~~ for the H₂, ~~and D₂, and Mu~~ + CH₄ reactions, ~~respectively and 72° for the Mu + CH₄ reaction~~. The larger skew angle means there will be less tunneling.⁸⁰

Figure 2 displays the corresponding transmission coefficients as a function of time. The non-unity long-time values indicate that even at the optimal barrier top (ξ^\ddagger) there is still significant recrossing. The RPMD values are lower than their classical counterparts, indicating larger recrossing. The Mu + CH₄ reaction has the largest recrossing. Some oscillations are also seen for both the classical and RPMD transmission coefficients of the Mu + CH₄ reaction, which is due to vibrational motion near the transition state, as seen before in the Mu + H₂ reactions.^{61, 63}

Interestingly, the RPMD transmission coefficients in Table 1 generally *increase* with temperature, suggesting more recrossing at low temperatures, as seen in previous RPMD studies.⁵⁹⁻⁶⁰ This is in contrast to the behavior of the classical transmission coefficients, which *decrease* with temperature (not shown). As Richardson and Althorpe pointed out,⁶⁴ in the deep tunneling region below the cross-over temperature, $T_c = \hbar\omega_b / 2\pi k_B$ in which ω_b is the imaginary frequency at the top of the reaction barrier, the excited modes of the ring polymer start to contribute to the optimum reaction coordinate. As a result, the centroid variable is no longer an optimal quantity for defining the dividing surface and the QTST rate coefficient becomes artificially large.⁶⁰ RPMD

compensates this by increasing recrossing at low temperatures to guarantee the independence in choosing the dividing surface. The calculated cross-over temperature (T_c) is approximately 341 K for all three isotopes as ω_b are almost identical for the three isotopes on this PES.

The calculated rate coefficients for the reactions of H/D/Mu + CH₄ as well as other quantities obtained in the RPMD calculations are listed in Table 1. It is interesting to note that the lighter isotopes have smaller rate coefficients than their heavier counterparts. These so-called “inverse KIEs” are primary isotope effect, due to the relative ZPEs in the reactant and product sides of the reaction, which can overwhelm the tunneling effects, are well established for these reactions.^{78, 81}

Figure 4 displays the comparison of the RPMD rate coefficients of the H + CH₄ reaction with experimental and previous theoretical results in the Arrhenius plot. The experimental rate coefficients for this reaction are quite scattered, but we will take the recently recommended values of Baulch *et al.*⁸ as the most reliable. In addition to the recommended values, we will also consider the experimental work of Kurylo *et al.*,³ because it is the only experiment that reported the H/D KIE, and the work of Sutherland *et al.*,⁶ whose recommendation is very close to that of Baulch *et al.*⁸ The agreement with the most recent experiment of Sutherland *et al.*⁶ is quite good, but the calculated rate coefficients are substantially smaller than those reported earlier by Kurylo *et al.*³ It is known that the latter might contain contributions from secondary reactions, such as H/D + CH₃, as discussed by the authors.³ These secondary reactions may consume the reactant atoms, making the observed rate coefficient fictitiously large. The overall agreement with

the latest recommendation of Baulch *et al.*⁸ is quite good, although the RPMD rate coefficients are a bit too small.

The RPMD rate coefficients are in good agreement with the MCTDH²⁹ and canonical variational transition-state theory with the μ OMT treatment of tunneling (CVT/ μ OMT) results,¹⁸ which were obtained on the same PES used in this work. Quantitatively, the RPMD rate coefficients are higher than the MCTDH values by less than 50%, while the differences from the μ OMT values are less than 10%. While the agreement between the RPMD and MCTDH rate coefficients is expected from the previous calculations,^{60, 62} its confirmation nonetheless is very comforting. The agreement with the CVT/ μ OMT results, on the other hand, confirmed a proper accounting of tunneling by the semi-classical μ OMT model. This conclusion is consistent with that reached by Pu and Truhlar on the validation of the CVT/ μ OMT model for the H + CH₄ reaction.⁵² We note in passing that the calculated rate coefficients on PES-2008¹⁷ differ significantly from the results, including CVT/ μ OMT,¹⁵ MCTDH,³⁰ and RPMD,⁶⁰ on an earlier PES (PES-2002),¹⁵ which underestimated the barrier height.

In Fig. 5, the comparison for the D + CH₄ rate coefficients is shown in the Arrhenius plot. The experimental data from Kurylo *et al.*³ are again significantly larger than all theoretical ones, which might stem from the same problem with the secondary reactions as discussed above. To our best knowledge, there has not been any more recent work on this reaction. Given the much smaller rate coefficients recommended by Baulch *et al.*⁸ and by Sutherland *et al.*⁶ for the H + CH₄ reaction, it is likely that the rate coefficient in the study of Kurylo *et al.*³ were also overestimated for the D + CH₄

reaction.²⁹ In other words, we believe that the theoretical rate coefficients are probably more accurate than their experimental counterparts.

Comparing with the theoretical results, it is clear that the agreement of the RPMD rate coefficient with the MCTDH results²⁹ remains quite good, despite the fact that the latter were computed on a different PES of Wu, Werner and Manthe.¹⁶ As pointed out by Schiffel and Manthe,³⁴ however, the two PESs yielded very similar rate coefficients for the H + CH₄ reaction. As a result, we conclude that the RPMD rate coefficients are also accurate for the D + CH₄ reaction. Similarly, the agreement between the RPMD and CVT/ μ OMT results remains excellent, providing further evidence for the accuracy of the semi-classical treatment of tunneling for this reaction.

Interestingly, the discrepancy between the RPMD and experimental rate coefficients for the Mu + CH₄ reaction is significant, as shown in the Arrhenius plot displayed in Fig. 6. The RPMD rate coefficients are 63%, 56%, and 35% of the experimental values at the three temperatures. Interestingly, most existing theoretical predictions^{42, 53-54} of the rate coefficients for the Mu + CH₄ reaction substantially underestimate the experiment. In particular, the CVT/ μ OMT calculations on the PES-2002 PES¹⁵ found the theoretical rate coefficients also significantly lower than the experimental ones, despite the fact that the calculated rate coefficients for the H/D + CH₄ reaction overestimate the experimental counterparts.⁵⁴

Interestingly, the RPMD rate coefficients are larger than the CVT/ μ OMT results obtained by us on the same PES-2008 using the same method in Ref. 18 as implemented in PolyRate.⁸² At the three temperatures, the RPMD rate coefficients are roughly two

times of their μ OMT counterparts. Although there has not been any MCTDH calculation for the ultralight isotope, it is likely that the discrepancy is due to the TST model, given the excellent agreement between RPMD and MCTDH rate coefficients for the H/D + CH₄ reactions, as well as the excellent agreement between RPMD rate coefficients and accurate quantum mechanical (QM) results for Mu + H₂ reaction.^{61, 63} Indeed, it is well known that reactions involving Mu are challenging for transition-state theory, as significant discrepancies between accurate quantum mechanical and TST rate coefficients have been observed in the Mu + H₂ reaction.^{79, 83} There are several possible sources of errors. The thick barrier and high ZPE of the products shown in Fig. 3 makes it unlikely that the tunneling plays a major role in this reaction. As a result, the semi-classical treatment of the tunneling effects is probably not responsible. On the other hand, there is the possibility that the errors are introduced in the harmonic approximation in calculating the partition functions. Note that the Mu-H frequency is close to 10,000 cm⁻¹, and the exclusion of anharmonicities could lead to large errors, even at low temperatures. This hypothesis is reinforced by the excellent agreement of the RPMD rate coefficients for the Mu + H₂ → MuH + H reaction with experimental and QM values, which suggests that the RPMD approach is accurate for reactions involving Mu.^{61, 63}

The KIEs are displayed in Fig. 6 for the three hydrogen isotopes. The experimental $k_{\text{H}}/k_{\text{D}}$ values were those of Kurylo *et al.*,³ while the $k_{\text{Mu}}/k_{\text{H}}$ values were obtained using the H + CH₄ recommended values by Sutherland *et al.*⁶ and the Mu + CH₄ data of Snooks *et al.*⁵ In addition to the MCTDH and CVT/ μ OMT results discussed above, the earlier CVT/ μ OMT results^{15, 53} and the more recent reduced-dimensional

quantum dynamics (RD-QD) results⁴² are also included. The RD-QD results were obtained on a different PES.

For k_H/k_D , the theoretical values all underestimate KIE, but within the experimental error bars. Interestingly, all the theoretical results are close to each other, despite of different methodology and PESs used in the calculations. The self-consistency certainly instills confidence in the theoretical results. Indeed, the experimental rate coefficient for the D + CH₄ reactions are likely overestimated due to secondary reactions as discussed above,³ which might be responsible for the discrepancy.

Similarly, most theoretical k_{Mu}/k_H values also underestimate the experimental KIEs, particularly at high temperatures. The only exception is the RD-QD results of Banks *et al.*⁴² The underestimation can be attributed to the fact that all calculated rate coefficients for the Mu + CH₄ reaction are much smaller than the measurements. Pu and Truhlar⁵³ have compiled a list of possible reasons for this discrepancy, which include (1) the Born-Oppenheimer approximation may fail for this ultralight isotope of H; (2) the PES might not be accurate enough; (3) the experiment contains significant errors; (4) significant errors are introduced by the semi-classical tunneling approximations; and (5) significant errors are introduced by the partition function calculations. These authors argued that the errors introduced by non-adiabatic corrections (reason 1) should not be larger than a factor of two, based on agreement in other reactions involved Mu. They also concluded that large experimental errors (reason 3) are also unlikely, given the small uncertainties in the measurement. In fact, it was argued by Snooks *et al.* that the experimental measurements for the Mu + CH₄ reaction are more reliable than those for the H/D + CH₄ reactions.⁵

It is worth noting that the excellent agreement between RPMD, QM, and experimental rate coefficients for the $\text{Mu} + \text{H}_2$ reaction^{61, 63, 79} clearly suggests that RPMD is capable of an accurate account for ZPE effects and proper treatment of tunneling effect. Thus, the RPMD data for the $\text{Mu} + \text{CH}_4$ reaction appears to suggest some errors in the semi-classical treatment for tunneling and/or in the partition functions used, evidenced by the differences from the CVT/ μ OMT results in Fig. 5. Since it is well established that the reaction involving Mu has little tunneling (reason 4),^{61, 63, 78} the errors are most likely due to the calculation of the reactant partition function (reason 5). We emphasize that the reactant partition function is not directly calculated in RPMD, but accurately accounted for in the PMF. However, the proper treatment of both in RPMD still does not account for the large discrepancy with experiment, as shown in Fig. 5. It thus follows that the errors stem most likely from the PES used in the calculations. It is known that the PES-2008 is an empirical PES calibrated with limited *ab initio* information.¹⁷ While it reproduces the rate coefficients for the $\text{H/D} + \text{CH}_4$ reactions well, subtle features such as the barrier shape and vibrational frequencies near the transition state might have a large impact on the rate coefficient for the ultralight isotope Mu.⁵³ Indeed, it has been shown that quantum dynamics on the PES-2008 produces different results from those on *ab initio* PESs.^{21, 43} Recent MCTDH calculations of the $\text{H} + \text{CH}_4$ rate coefficients on different PESs also uncovered significant differences.³⁵ There are several *ab initio* global PESs available^{19, 21} and we plan to examine the RPMD calculations on these more accurate PESs in the near future.

V. Conclusions

In this work, we apply a full-dimensional approximate quantum mechanical method, namely ring-polymer molecular dynamics (RPMD), to calculate the rate coefficient and KIEs for hydrogen abstraction reactions of methane by hydrogen and its isotopes (D and Mu). Such studies not only help to establish the validity of the RPMD approach to thermal rate coefficients in reactions involving polyatomic reactants, but also to assess the commonly used transition-state theory with semi-classical tunneling corrections. For the first objective, it is shown that the RPMD rate coefficients for the H/D + CH₄ reactions are in excellent agreement with the established MCTDH results obtained on the same PES, thus providing additional evidence in support of the validity of the RPMD approach. The accuracy, robustness, and efficiency of the RPMD approach to rate coefficient calculations demonstrated in this and other studies have established its applicability in gas phase kinetics.

Interestingly, the comparison of RPMD and CVT/ μ OMT rate coefficients provide a mixed outcome. For the H/D + CH₄ reactions, the agreement is quite good, thus suggesting an accurate account of the tunneling by the semi-classical model. However, the poor agreement between the two for the Mu + CH₄ reaction indicates possible errors in the transition-state theory results. The source of errors stem presumably from neglect of anharmonicities in calculating the partition functions.

The overall agreement with experimental rate coefficient is good for the H + CH₄ reaction, particularly with the latest measurement by Sutherland *et al.*⁶ and the recommended values of Baulch *et al.*⁸ However, the agreement with the earlier measurement of Kurylo *et al.*³ is less satisfactory for both H and D + CH₄ reactions, presumably due to the involvement of secondary reactions in the experiment. The theory-

experiment agreement for the $\text{Mu} + \text{CH}_4$ reaction is, on the other hand, worse, although the RPMD results are closer to the experimental results of Snooks *et al.*⁵ than the CVT/ μ OMT counterparts on the same PES. The large discrepancy is tentatively attributed to the inaccuracy of the PES used in the calculations.

There are still significant discrepancies between calculated and measured kinetic isotope effects for this important reaction. The errors in $k_{\text{H}}/k_{\text{D}}$ can be attributed to the uncertainties in the experimental measurement, but the $k_{\text{Mu}}/k_{\text{H}}$ is probably due to inaccuracies in the PES, as mentioned above. This observation suggests that the rate coefficient for the ultralight $\text{Mu} + \text{CH}_4$ reaction is a much more stringent test of the PES, particularly the transition-state region, than its heavier isotopes. Future calculations with *ab initio* based PESs will be needed to resolve this important issue.

Acknowledgements: YL, JL, HG, and WHG were supported by the Department of Energy (DE-FG02-05ER15694 to HG and DE-FG02-98ER14914 to WHG). YVS acknowledges the support of a Combustion Energy Research Fellowship through the Combustion Energy Frontier Research Center, an Energy Frontier Research Center funded by the U.S. Department of Energy, Office of Basic Energy Sciences under Award Number DE-SC0001198. HG thanks Joaquin Espinosa-García for sending us some unpublished data and Don Fleming, David Manolopoulos, and Don Truhlar for several useful discussions.

References:

- 1 W. C. Gardiner, *Combustion Chemistry*. (Springer, Berlin, 1984).
- 2 M. J. Kurylo and R. B. Timmons, *J. Chem. Phys.* **50**, 5076 (1969).
- 3 M. J. Kurylo, G. A. Hollinden and R. B. Timmons, *J. Chem. Phys.* **52**, 1773 (1970).
- 4 M. J. Rabinowitz, J. W. Sutherland, P. M. Patterson and R. B. Klemm, *J. Phys. Chem.* **95**, 674 (1991).
- 5 R. Snooks, D. J. Arseneau, D. G. Fleming, M. Senba, J. J. Pan, M. Shelley and S. Baer, *J. Chem. Phys.* **102**, 4860 (1995).
- 6 J. W. Sutherland, M. C. Su and J. V. Michael, *Int. J. Chem. Kinet.* **33**, 669 (2001).
- 7 M. G. Bryukov, I. R. Slagle and V. D. Knyazev, *J. Phys. Chem. A* **105**, 3107 (2001).
- 8 D. L. Baulch, C. T. Bowman, C. J. Cobos, R. A. Cox, T. Just, J. A. Kerr, M. J. Pilling, D. Stocker, J. Troe, W. Tsang, R. W. Walker and J. Warnatz, *J. Phys. Chem. Ref. Data* **34**, 757 (2005).
- 9 G. J. Germann, Y.-D. Huh and J. J. Valentini, *J. Chem. Phys.* **96**, 1957 (1992).
- 10 J. P. Camden, H. A. Bechtel, D. J. A. Brown, M. R. Martin, R. N. Zare, W. Hu, G. Lendvay, D. Troya and G. C. Schatz, *J. Am. Chem. Soc.* **127**, 11898 (2005).
- 11 W. Zhang, Y. Zhou, G. Wu, Y. Lu, H. Pan, B. Fu, Q. Shuai, L. Liu, S. Liu, L. Zhang, B. Jiang, D. Dai, S.-Y. Lee, Z. Xie, B. J. Braams, J. M. Bowman, M. A. Collins, D. H. Zhang and X. Yang, *Proc. Natl. Acad. Sci. USA* **107**, 12782 (2010).
- 12 S. C. Althorpe and D. C. Clary, *Annu. Rev. Phys. Chem.* **54**, 493 (2003).
- 13 T. V. Albu, J. Espinosa-García and D. G. Truhlar, *Chem. Rev.* **107**, 5101 (2007).
- 14 J. C. Corchado, J. Espinosa-García, O. Roberto-Neto, Y.-Y. Chuang and D. G. Truhlar, *J. Phys. Chem. A* **102**, 4899 (1998).
- 15 J. Espinosa-Garcia, *J. Chem. Phys.* **116**, 10664 (2002).
- 16 T. Wu, H.-J. Werner and U. Manthe, *J. Chem. Phys.* **124**, 164307 (2006).
- 17 J. C. Corchado, J. L. Bravo and J. Espinosa-Garcia, *J. Chem. Phys.* **130**, 184314 (2009).
- 18 J. Espinosa-Garcia, G. Nyman and J. C. Corchado, *J. Chem. Phys.* **130**, 184315 (2009).
- 19 X. Zhang, B. J. Braams and J. M. Bowman, *J. Chem. Phys.* **124**, 021104 (2006).
- 20 Z. Xie, J. M. Bowman and X. Zhang, *J. Chem. Phys.* **125**, 133120 (2006).
- 21 Y. Zhou, B. Fu, C. Wang, M. A. Collins and D. H. Zhang, *J. Chem. Phys.* **134**, 064323 (2011).
- 22 H.-D. Meyer, U. Manthe and L. S. Cederbaum, *Chem. Phys. Lett.* **165**, 73 (1990).
- 23 U. Manthe, H.-D. Meyer and L. S. Cederbaum, *J. Chem. Phys.* **97**, 9062 (1992).
- 24 F. Huarte-Larrañaga and U. Manthe, *J. Chem. Phys.* **113**, 5115 (2000).
- 25 F. Huarte-Larrañaga and U. Manthe, *J. Phys. Chem. A* **105**, 2522 (2001).
- 26 J. M. Bowman, D. Wang, X. Huang, F. Huarte-Larrañaga and U. Manthe, *J. Chem. Phys.* **114**, 9683 (2001).
- 27 F. Huarte-Larrañaga and U. Manthe, *J. Chem. Phys.* **116**, 2863 (2002).
- 28 T. Wu, H.-J. Werner and U. Manthe, *Science* **306**, 2227 (2004).

- 29 R. Van Harrevelt, G. Nyman and U. Manthe, *J. Chem. Phys.* **126**, 084303 (2007).
- 30 S. Andersson, G. Nyman, A. Arnaldsson, U. Manthe and H. Jonsson, *J. Phys. Chem. A* **113**, 4468 (2009).
- 31 G. Schiffel and U. Manthe, *J. Chem. Phys.* **133**, 174124 (2010).
- 32 G. Schiffel and U. Manthe, *J. Chem. Phys.* **132**, 084103 (2010).
- 33 G. Schiffel and U. Manthe, *J. Chem. Phys.* **132**, 191101 (2010).
- 34 G. Schiffel and U. Manthe, *J. Phys. Chem. A* **114**, 9617 (2010).
- 35 R. Welsch and U. Manthe, *J. Chem. Phys.* **137**, 244106 (2012).
- 36 H.-G. Yu and G. Nyman, *J. Chem. Phys.* **111**, 3508 (1999).
- 37 M.-L. Wang, Y.-M. Li, J. Z. H. Zhang and D. H. Zhang, *J. Chem. Phys.* **113**, 1802 (2000).
- 38 D. Wang and J. M. Bowman, *J. Chem. Phys.* **115**, 2055 (2001).
- 39 J. Palma and D. C. Clary, *J. Phys. Chem. A* **106**, 8256 (2002).
- 40 M. Yang, D. H. Zhang and S.-Y. Lee, *J. Chem. Phys.* **117**, 9539 (2002).
- 41 L. Zhang, Y. Lu, S.-Y. Lee and D. H. Zhang, *J. Chem. Phys.* **127**, 234313 (2007).
- 42 S. T. Banks, C. S. Tautermann, S. M. Remmert and D. C. Clary, *J. Chem. Phys.* **131**, 044111 (2009).
- 43 Y. Zhou, C. Wang and D. H. Zhang, *J. Chem. Phys.* **135**, 024313 (2011).
- 44 R. Liu, H. Xiong and M. Yang, *J. Chem. Phys.* **137**, 174113 (2012).
- 45 S. Liu, J. Chen, Z. Zhang and D. H. Zhang, *J. Chem. Phys.* **138**, 011101 (2013).
- 46 J. M. Bowman, *J. Phys. Chem.* **95**, 4960 (1991).
- 47 U. Manthe, *Mole. Phys.* **109**, 1415 (2011).
- 48 D. G. Truhlar and B. C. Garrett, *Annu. Rev. Phys. Chem.* **35**, 159 (1984).
- 49 D. G. Truhlar, A. D. Issacson and B. C. Garrett, in *Theory of Chemical Reaction Dynamics*, edited by M. Bear (CRC, Boca Raton, 1985), pp. 65-137.
- 50 T. L. Nguyen, J. F. Stanton and J. R. Barker, *Chem. Phys. Lett.* **499**, 9 (2010).
- 51 D. G. Truhlar, B. C. Garrett and S. J. Klippenstein, *J. Phys. Chem.* **100**, 12771 (1996).
- 52 J. Pu and D. G. Truhlar, *J. Chem. Phys.* **117**, 1479 (2002).
- 53 J. Pu and D. G. Truhlar, *J. Chem. Phys.* **117**, 10675 (2002).
- 54 J. Espinosa-García, *Phys. Chem. Chem. Phys.* **10**, 1277 (2008).
- 55 Y. Zhao, T. Yamamoto and W. H. Miller, *J. Chem. Phys.* **120**, 3100 (2004).
- 56 Y. V. Suleimanov, J. W. Allen and W. H. Green, *Comput. Phys. Comm.* **184**, 833 (2013).
- 57 D. Chandler and P. G. Wolynes, *J. Chem. Phys.* **74**, 4078 (1981).
- 58 I. R. Craig and D. E. Manolopoulos, *J. Chem. Phys.* **121**, 3368 (2004).
- 59 R. Colleparado-Guevara, Y. V. Suleimanov and D. E. Manolopoulos, *J. Chem. Phys.* **130**, 174713 (2009).
- 60 Y. V. Suleimanov, R. Colleparado-Guevara and D. E. Manolopoulos, *J. Chem. Phys.* **134**, 044131 (2011).
- 61 R. Pérez de Tudela, F. J. Aoiz, Y. V. Suleimanov and D. E. Manolopoulos, *J. Phys. Chem. Lett.* **3**, 493 (2012).
- 62 Y. Li, Y. V. Suleimanov, M. Yang, W. H. Green and H. Guo, *J. Phys. Chem. Lett.* **4**, 48 (2013).

- 63 Y. V. Suleimanov, R. Pérez de Tudela, P. G. Jambrina, J. F. Castillo, V. Sáez-Rábanos, D. E. Manolopoulos and F. J. Aoiz, *Phys. Chem. Chem. Phys.* **in press** (2013)(doi: 10.1039/C2CP44364C).
- 64 J. O. Richardson and S. C. Althorpe, *J. Chem. Phys.* **131**, 214106 (2009).
- 65 W. H. Miller, S. D. Schwartz and J. W. Tromp, *J. Chem. Phys.* **79**, 4889 (1983).
- 66 I. R. Craig and D. E. Manolopoulos, *J. Chem. Phys.* **122**, 084106 (2005).
- 67 I. R. Craig and D. E. Manolopoulos, *J. Chem. Phys.* **123**, 034102 (2005).
- 68 C. H. Bennett, in *Algorithms for Chemical Computations, ACS Symposium Series*, edited by R. E. Christofferson (ACS, 1977), Vol. 46.
- 69 D. Chandler, *J. Chem. Phys.* **68**, 2959 (1978).
- 70 D. Frenkel and B. Smit, *Understanding Molecular Simulation, Second Edition: From Algorithms to Applications* (Academic Press, San Diego, 2002).
- 71 J. B. Anderson, *Adv. Chem. Phys.* **91**, 381 (1995).
- 72 R. Collepardo-Guevara, I. R. Craig and D. E. Manolopoulos, *J. Chem. Phys.* **128**, 144502 (2008).
- 73 J. Kästner and W. Thiel, *J. Chem. Phys.* **123**, 144104 (2005).
- 74 T. E. Markland and D. E. Manolopoulos, *J. Chem. Phys.* **129**, 024105 (2008).
- 75 M. Ceriotti, M. Parrinello, T. E. Markland and D. E. Manolopoulos, *J. Chem. Phys.* **133**, 124104 (2010).
- 76 H. C. Andersen, *J. Chem. Phys.* **72**, 2384 (1980).
- 77 J. P. Ryckaert, G. Ciccotti and H. J. Berendsen, *J. Comput. Phys.* **23**, 327 (1977).
- 78 D. K. Bondi, D. C. Clary, J. N. L. Connor, B. C. Garrett and D. G. Truhlar, *J. Chem. Phys.* **76**, 4986 (1982).
- 79 D. G. Fleming, D. J. Arseneau, O. Sukhorukov, J. H. Brewer, S. L. Mielke, G. C. Schatz, B. C. Garrett, K. A. Peterson and D. G. Truhlar, *Science* **331**, 448 (2011).
- 80 D. G. Truhlar and M. S. Gordon, *Science* **249**, 491 (1990).
- 81 G. C. Schatz, A. F. Wagner and T. H. Dunning Jr., *J. Phys. Chem.* **88**, 221 (1984).
- 82 J. C. Corchado, Y.-Y. Chuang, P. L. Fast, W.-P. Hu, Y.-P. Liu, G. C. Lynch, K. A. Nguyen, C. F. Jackels, A. Fernandez Ramos, B. A. Ellingson, B. J. Lynch, J. Zheng, V. S. Melissas, J. Villà, I. Rossi, E. L. Coitiño, J. Pu, T. V. Albu, R. Steckler, B. C. Garrett, A. D. Isaacson and D. G. Truhlar, (University of Minnesota, Minneapolis, 2007).
- 83 D. G. Fleming, D. J. Arseneau, O. Sukhorukov, J. H. Brewer, S. L. Mielke, D. G. Truhlar, G. C. Schatz, B. C. Garrett and K. A. Peterson, *J. Chem. Phys.* **135**, 184310 (2011).

Fig. 1 Potentials of mean force (PMF) of the H/D/Mu + CH₄ reactions at 626 K.

Fig. 2 Transmission coefficients of the H/D/Mu + CH₄ reactions at 626 K.

Fig. 3 Minimum energy path (black solid line) and the adiabatic curve for the ground vibrational state (red dashed line) for the reaction H + CH₄ and Mu + CH₄ along the reaction coordinate.

Fig. 4 Comparison among RPMD, MCTDH,³⁴ CVT/ μ OMT,¹⁸ and experimental rate coefficients for the H + CH₄ reaction. Experimental data are taken from Kurylo *et al.*,³ Sutherland *et al.*,⁶ and the recommended values from Baulch *et al.*⁸

Fig. 4 Comparison among RPMD, MCTDH,²⁹ CVT/ μ OMT,¹⁸ and experimental rate coefficients³ for the D + CH₄ reaction.

Fig. 5 Comparison among RPMD, CVT/ μ OMT (this work), and experimental rate coefficients⁵ for the Mu + CH₄ reaction.

Fig. 6 Comparison between calculated and measured KIEs ($k_{\text{H}}/k_{\text{D}}$ in the upper panel and $k_{\text{Mu}}/k_{\text{H}}$ in the lower panel). Upper panel: comparison of $k_{\text{H}}/k_{\text{D}}$ between RPMD, MCTDH,²⁹ CVT/ μ OMT (PES-2002),¹⁵ CVT/ μ OMT (MCGS-SRP),⁵³ CVT/ μ OMT (PES-2008),¹⁸ and reduced-dimensional quantum dynamics (RD-QD) results from Banks *et al.*, who used a different RD PES.⁴² Lower panel: comparison of between $k_{\text{Mu}}/k_{\text{H}}$ RPMD, CVT/ μ OMT (MCGS-SRP),⁵³ CVT/ μ OMT (PES-2008) done in this work, and RD-QD results from Banks *et al.*⁴²

Fig. 1

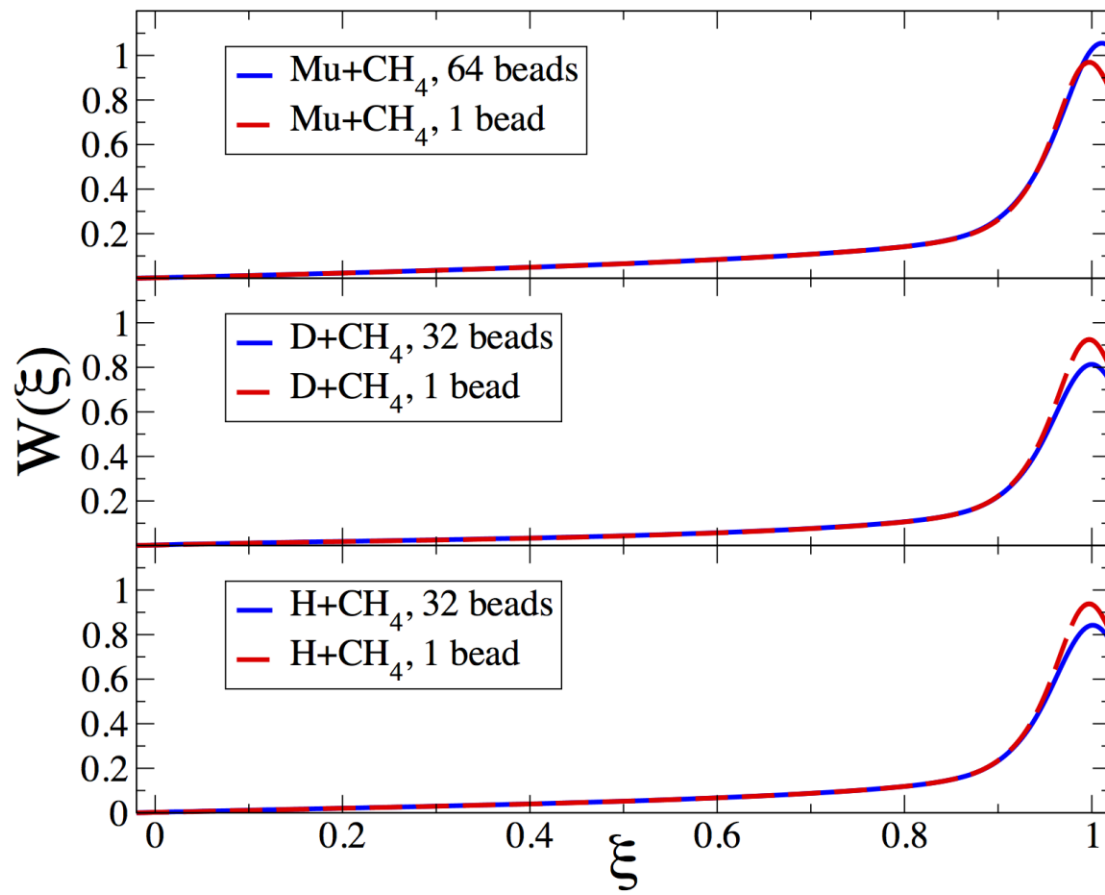


Fig. 2

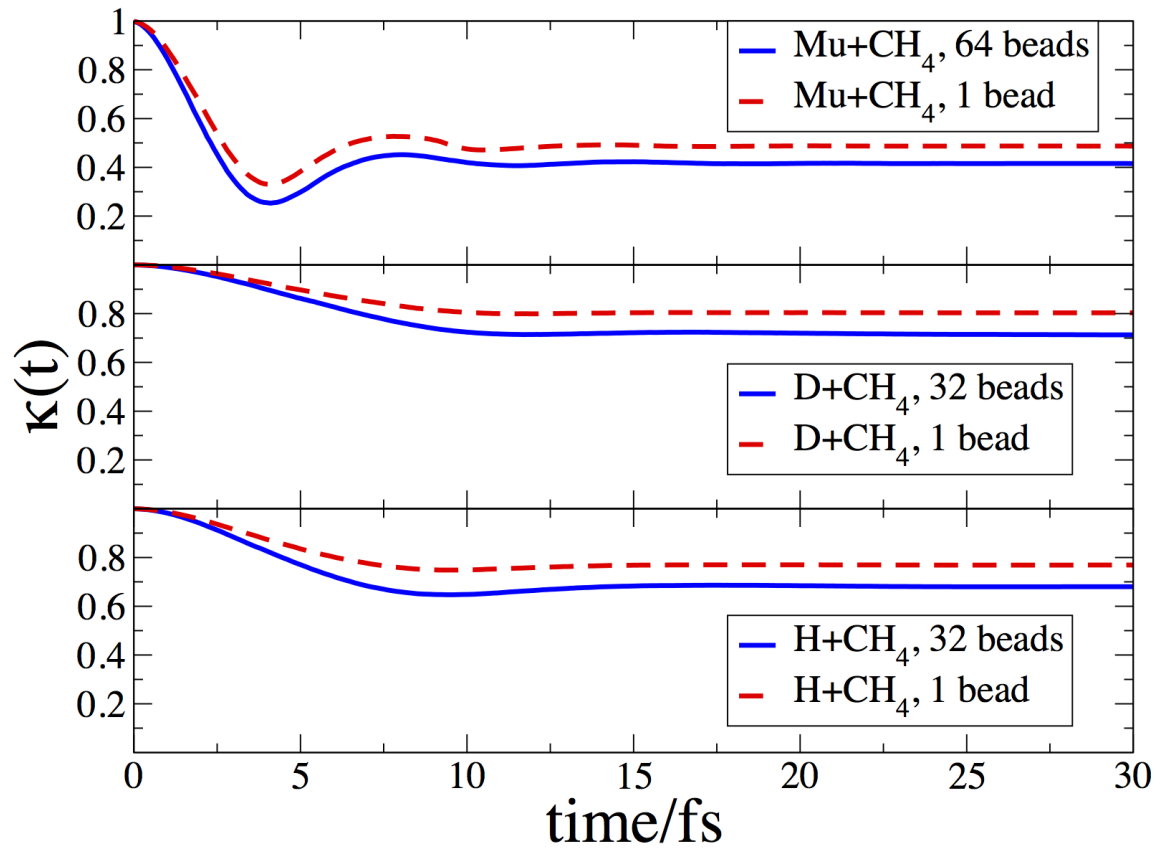


Fig. 3

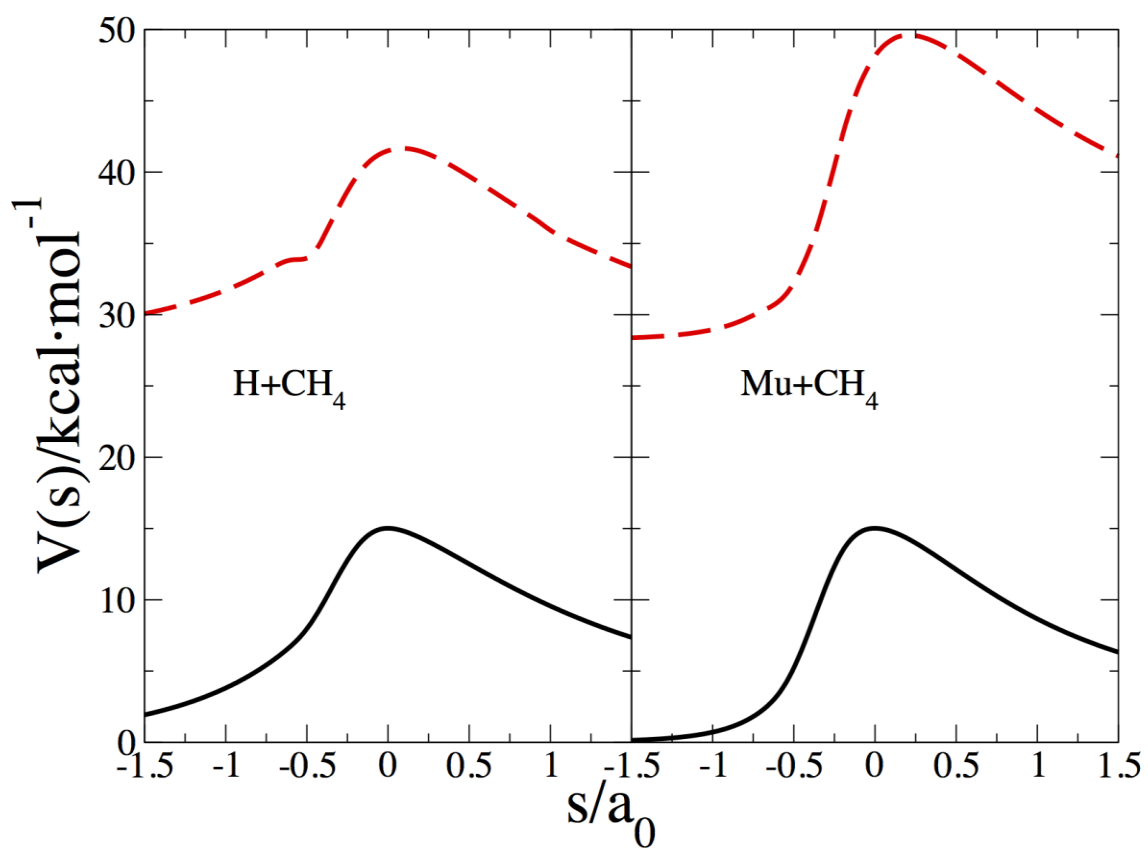


Fig. 4

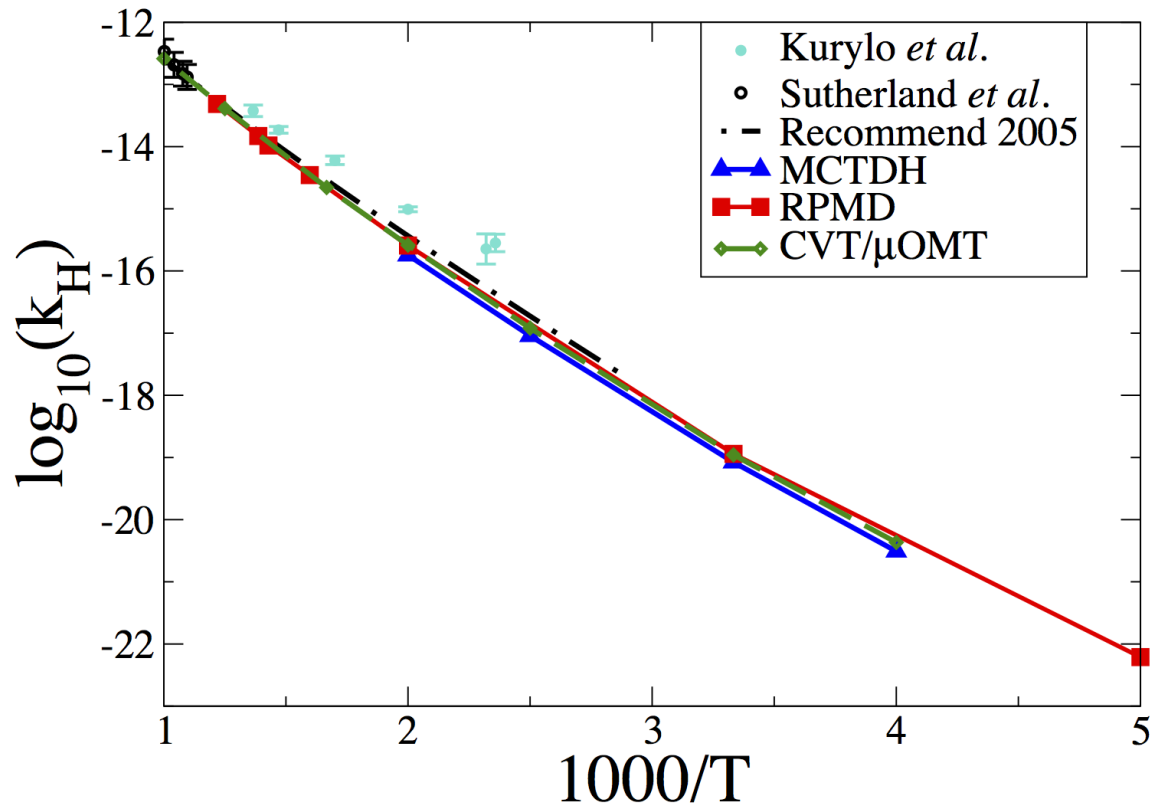


Fig. 5

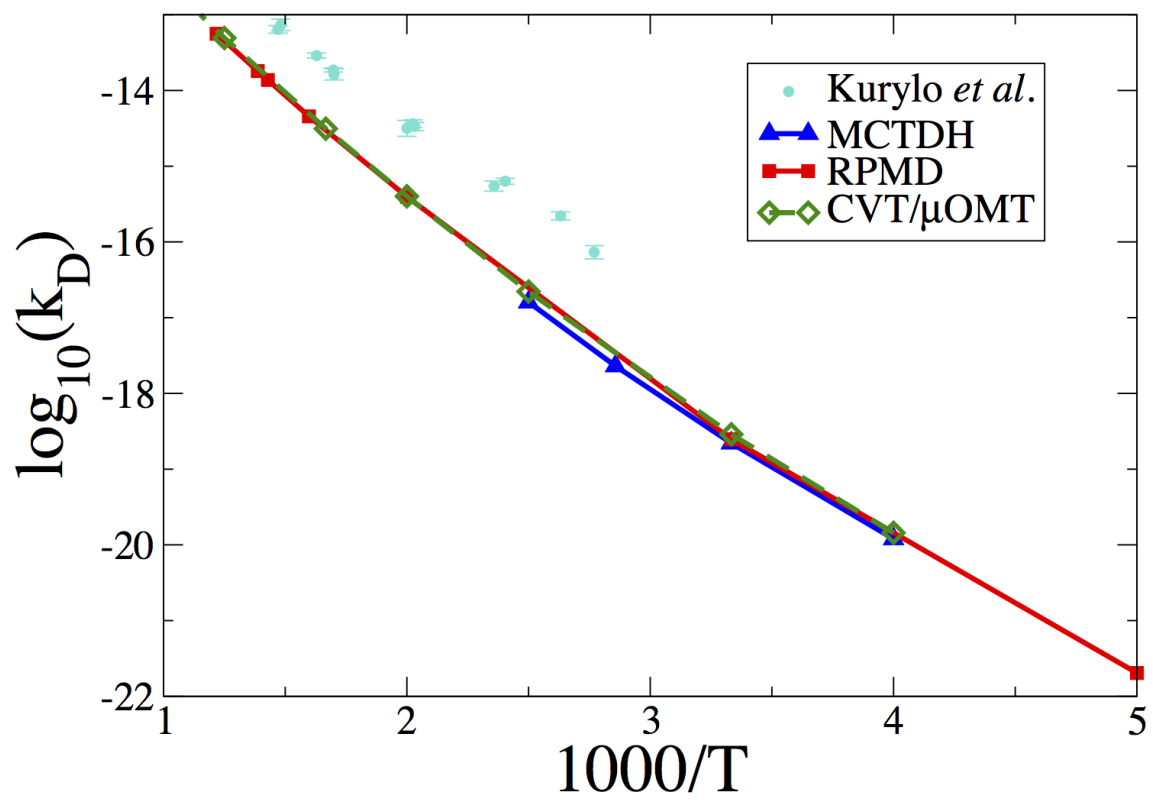


Fig. 6

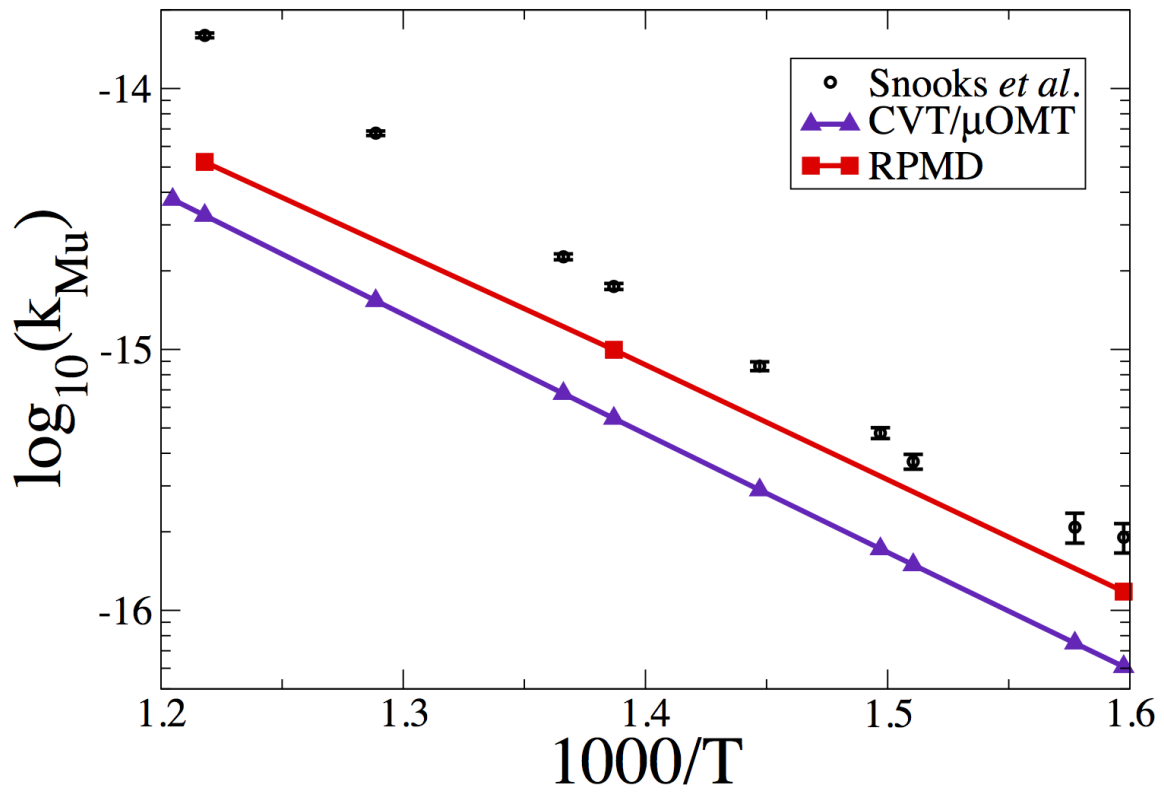


Fig. 7

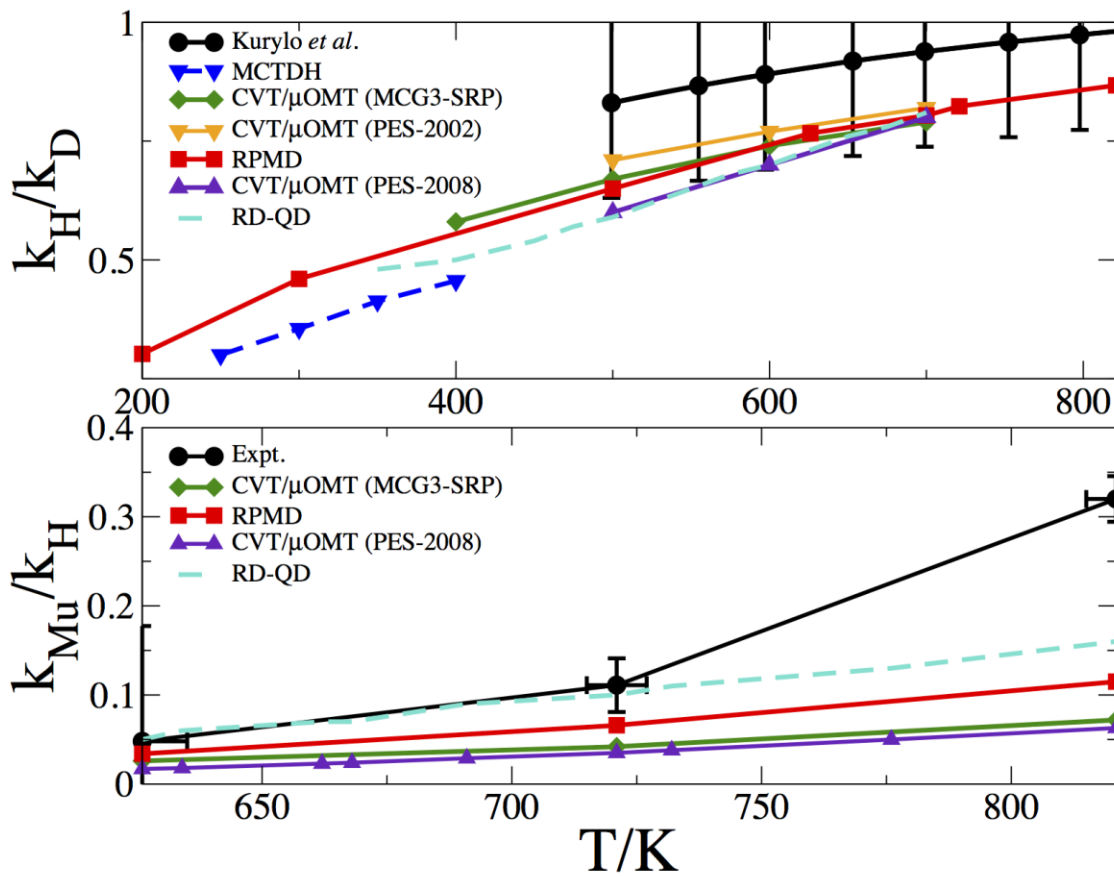


Table 1. Summary of RPMD results for the H/D/Mu + CH₄ reactions using PES-2008.¹⁷ ξ^\ddagger and $\Delta G(\xi^\ddagger)$ (in eV) are the peak position and barrier height of the PMF curve along the reaction coordinate ξ . κ is the plateau value of the transmission coefficient. k_{QTST} and k_{RPMD} are the centroid density QTST rate coefficients and the corresponding RPMD rate coefficients, respectively. All the rate coefficients are in the unit cm³molecule⁻¹s⁻¹.

H+CH ₄ , T/K	200	300	500	626	700	721	821
N_{beads}	128	128	64	32	32	32	32
ξ^\ddagger	1.014	1.007	1.003	1.001	1.000	1.000	0.999
$\Delta G(\xi^\ddagger)$	0.565	0.660	0.780	0.842	0.877	0.886	0.930
k_{QTST}	1.01E-22	1.73E-19	3.81E-16	5.13E-15	1.57E-14	2.11E-14	6.86E-14
κ	0.611	0.660	0.674	0.680	0.694	0.702	0.707
k_{RPMD}	6.15E-23	1.14E-19	2.57E-16	3.49E-15	1.09E-14	1.48E-14	4.85E-14
$k_{\text{MCTDH}}^{\text{a}}$	--	8.40E-20	1.80E-16	--	--	--	--
$k_{\text{CVT}\mu\text{OMT}}^{\text{b}}$	--	1.10E-19	2.60E-16	--	--	--	--
$k_{\text{expt.}}^{\text{c}}$	--	--	3.67±0.73E-16	4.49±0.90E-15	1.34±0.27E-14	1.77±0.35E-14	5.52±1.10E-14
D+CH ₄ , T/K	200	300	500	626	700	721	821
N_{beads}	128	128	64	32	32	32	32
ξ^\ddagger	1.011	1.006	1.001	1.000	0.999	0.999	0.998
$\Delta G(\xi^\ddagger)$	0.539	0.633	0.747	0.813	0.846	0.855	0.900
k_{QTST}	3.27E-22	3.65E-19	5.68E-16	6.38E-15	1.90E-14	2.50E-14	7.70E-14
κ	0.621	0.679	0.695	0.713	0.715	0.719	0.727
k_{RPMD}	2.03E-22	2.48E-19	3.95E-16	4.55E-15	1.36E-14	1.80E-14	5.59E-14
$k_{\text{MCTDH}}^{\text{d}}$	--	2.20E-19	--	--	--	--	--
$k_{\text{CVT}\mu\text{OMT}}^{\text{b}}$	--	2.88E-19	4.00E-16	--	--	--	--
$k_{\text{expt.}}^{\text{e}}$	--	--	1.06±0.64E-15	1.00±0.57E-14	2.57±1.42E-14	3.24±1.79E-14	8.32±4.48E-14
Mu + CH ₄ T/K	200	300	500	626	700	721	821
N_{beads}	--	--	--	128	--	128	64
ξ^\ddagger	--	--	--	1.011	--	1.010	1.008
$\Delta G(\xi^\ddagger)$	--	--	--	1.056	--	1.090	1.125
k_{QTST}	--	--	--	2.85E-16	--	2.28E-15	1.33E-14
κ	--	--	--	0.417	--	0.428	0.419
k_{RPMD}	--	--	--	1.19E-16	--	9.76E-16	5.58E-15
$k_{\text{CVT}\mu\text{OMT}}^{\text{f}}$	--	2.69E-24	8.14E-19	6.08E-17	2.97E-16	5.44E-16	3.26E-15
$k_{\text{expt.}}^{\text{g}}$	--	--	--	1.90±0.245E-16	--	1.74±0.046E-15	1.60±0.033E-14

- ^a: Ref. ³⁴ using PES-2008.¹⁷
- ^b: Ref. ¹⁸ using PES-2008.¹⁷
- ^c: Recommended by Baulch *et al.*⁸
- ^d: Ref. ²⁹ using the PES of Wu, Werner and Manthe.²⁸
- ^e: Ref. ³.
- ^f: This work using PES-2008.¹⁷
- ^g: Ref. ⁵.